Morphoelastic Modelling of Skin Burns with IGA

Antonio Barion

TU Delft, MSc Applied Mathematics

June 4, 2020

Content

1. Motivation
2. Concept of Morphoelasticity
3. 1D Morphoelasticity
4. 2D Viscoelasticity
5. 2D Morphoelaticity
6. Extended Multi-Species Model
7. Future Work

Content

1. Motivation
2. Concept of Morphoelasticity
3. 1D Morphoelasticity
4. 2D Viscoelasticity
5. 2D Morphoelaticity
6. Extended Multi-Species Model
7. Future Work

Skin Burns and Scarring

- Scarred skin tissue does not maintain the same mechanical properties of healthy skin. This is particularly relevant in skin burns where the damaged area can be very extensive and lead to serious impediments for the patient.

Skin Burns and Scarring

- Scarred skin tissue does not maintain the same mechanical properties of healthy skin. This is particularly relevant in skin burns where the damaged area can be very extensive and lead to serious impediments for the patient.
- The healing and scarring process of skin is very complex. It is therefore difficult to predict its outcome.

Skin Burns and Scarring

- Scarred skin tissue does not maintain the same mechanical properties of healthy skin. This is particularly relevant in skin burns where the damaged area can be very extensive and lead to serious impediments for the patient.
- The healing and scarring process of skin is very complex. It is therefore difficult to predict its outcome.
- Mathematical modelling and simulation can clarify the influence which certain parameters have on the healing process.

Skin Burns and Scarring

- Scarred skin tissue does not maintain the same mechanical properties of healthy skin. This is particularly relevant in skin burns where the damaged area can be very extensive and lead to serious impediments for the patient.
- The healing and scarring process of skin is very complex. It is therefore difficult to predict its outcome.
- Mathematical modelling and simulation can clarify the influence which certain parameters have on the healing process.
- End goal is to devise an ‘optimal’ treatment approach for skin burns. This is only possible through thorough understanding of the underlying processes.

Content

1. Motivation
2. Concept of Morphoelasticity
3. 1D Morphoelasticity
4. 2D Viscoelasticity
5. 2D Morphoelaticity
6. Extended Multi-Species Model
7. Future Work

- Tissue deformation of healing burns has both plastic (permanent) and elastic (temporary) components. This can lead to the formation of residual stresses in the tissue at the end of the healing process.

- Tissue deformation of healing burns has both plastic (permanent) and elastic (temporary) components. This can lead to the formation of residual stresses in the tissue at the end of the healing process.
- We couple an elastic model with an evolving zero stress state. This state evolution will be described by the evolution equations of strain.

Content

1. Motivation
2. Concept of Morphoelasticity
3. 1D Morphoelasticity
4. 2D Viscoelasticity
5. 2D Morphoelaticity
6. Extended Multi-Species Model
7. Future Work

Equations

$$\begin{cases} \sigma = \mu \dfrac{\partial v}{\partial x} + E\varepsilon, \\ \dfrac{D(\rho v)}{Dt} + \rho v \dfrac{\partial v}{\partial x} = \dfrac{\partial \sigma}{\partial x} + F_b \quad \text{in } \Omega_t \times [0,T] \quad (\text{momentum}) \ , \\ \dfrac{D\varepsilon}{Dt} + (\varepsilon - 1)\dfrac{\partial v}{\partial x} = -g \quad \text{in } \Omega_t \times [0,T] \quad (\text{strain}) \ , \\ v = \dfrac{Du}{Dt}. \end{cases} \tag{1}$$

Equations are discretized in space using linear FE and in time using backward Euler (implicit). In our case we have $g = \zeta\varepsilon$.
Note: The operator D/Dt represents the material derivative:
$D()/Dt = \partial()/\partial t + v \cdot \nabla()$.
We will be using a moving mesh method.

Example

Example of tissue deforming under contracting forces acting until $t = 22$, where $\zeta = 0$ represent purely elastic response.

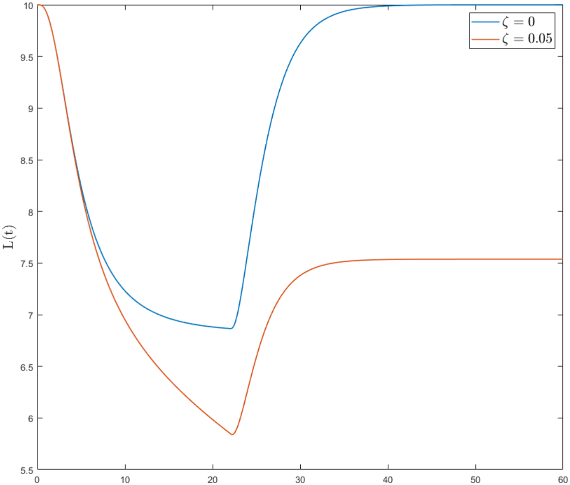

Content

1. Motivation
2. Concept of Morphoelasticity
3. 1D Morphoelasticity
4. 2D Viscoelasticity
5. 2D Morphoelaticity
6. Extended Multi-Species Model
7. Future Work

Equations

As an intermediate step before 2D-morphoelasticity we first tackled 2D viscoelasticity as it has the same momentum equations but simpler strain equations.

$$
\begin{cases}
\overline{\overline{\boldsymbol{\sigma}}} = \mu_1 \operatorname{sym}(\nabla \boldsymbol{v}) + \mu_2 (\nabla \cdot \boldsymbol{v}) \overline{\overline{\boldsymbol{I}}} + \dfrac{E\sqrt{\rho}}{1+\nu} \left(\overline{\overline{\boldsymbol{\varepsilon}}} + \dfrac{\nu}{1-2\nu} \operatorname{Tr}(\overline{\overline{\boldsymbol{\varepsilon}}}) \overline{\overline{\boldsymbol{I}}} \right), \\
\dfrac{D(\rho \boldsymbol{v})}{Dt} + \rho \boldsymbol{v} (\nabla \cdot \boldsymbol{v}) = \nabla \cdot \overline{\overline{\boldsymbol{\sigma}}} + \boldsymbol{f} \qquad \text{in } \Omega_t \times [0,T], \\
\overline{\overline{\boldsymbol{\varepsilon}}} = \dfrac{1}{2} \left(\nabla \boldsymbol{u} + (\nabla \boldsymbol{u})^T \right) \qquad \text{in } \Omega_t \times [0,T], \\
\dfrac{D\boldsymbol{u}}{Dt} = \boldsymbol{v}.
\end{cases}
\tag{2}
$$

Equations are discretized in space using quadrilateral bilinear FE and in time using backward Euler (implicit).

Example

Tissue under shear and contracting forces along the x-axis. We see the deformation of a subdomain in the centre of the tissue.

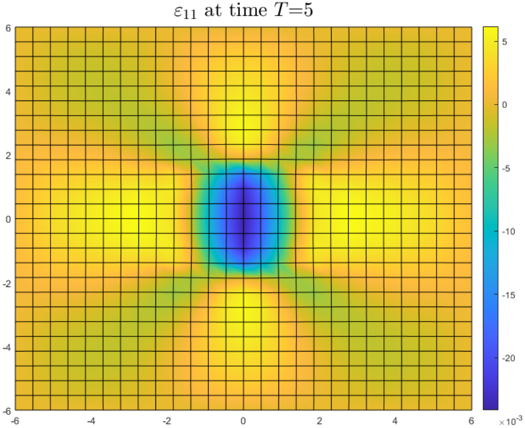

Figure: ε_{11} in our modelled tissue under contracting forces.

Example

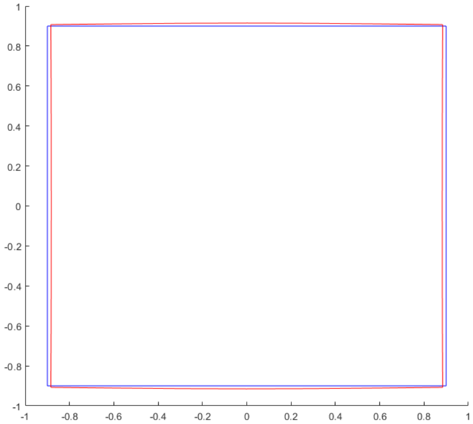

Figure: Contracting forces along x-axis. Subdomain at $t = 0$ in blue and at $t = 5$ in red.

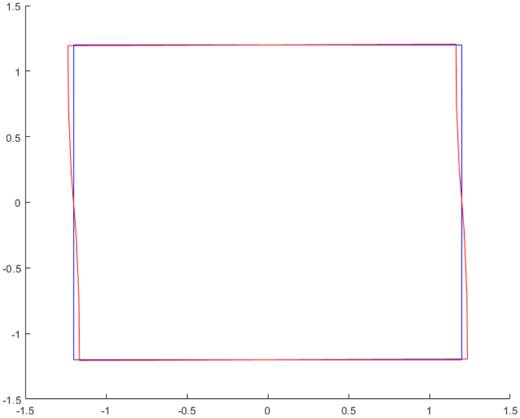

Figure: Shear forces along x-axis. Subdomain at $t = 0$ in blue and at $t = 5$ in red.

Content

1. Motivation
2. Concept of Morphoelasticity
3. 1D Morphoelasticity
4. 2D Viscoelasticity
5. 2D Morphoelaticity
6. Extended Multi-Species Model
7. Future Work

Equations

$$\begin{cases} \overline{\overline{\boldsymbol{\sigma}}} = \mu_1 \operatorname{sym}(\nabla \boldsymbol{v}) + \mu_2 (\nabla \cdot \boldsymbol{v}) \overline{\overline{\boldsymbol{I}}} + \dfrac{E\sqrt{\rho}}{1+\nu} \left(\overline{\overline{\boldsymbol{\varepsilon}}} + \dfrac{\nu}{1-2\nu} \operatorname{Tr}(\overline{\overline{\boldsymbol{\varepsilon}}}) \overline{\overline{\boldsymbol{I}}} \right), \\ \dfrac{D(\rho \boldsymbol{v})}{Dt} + \rho \boldsymbol{v} (\nabla \cdot \boldsymbol{v}) = \nabla \cdot \overline{\overline{\boldsymbol{\sigma}}} + \boldsymbol{f} \quad \text{in } \Omega_t \times [0,T], \\ \dfrac{D\overline{\overline{\boldsymbol{\varepsilon}}}}{Dt} + \overline{\overline{\boldsymbol{\varepsilon}}} \operatorname{skw}(\nabla \boldsymbol{v}) - \operatorname{skw}(\nabla \boldsymbol{v}) \overline{\overline{\boldsymbol{\varepsilon}}} + \big(\operatorname{Tr}(\overline{\overline{\boldsymbol{\varepsilon}}}) - 1 \big) \operatorname{sym}(\nabla \boldsymbol{v}) = -\overline{\overline{\boldsymbol{g}}} \\ \text{in } \Omega_t \times [0,T], \\ \dfrac{D\boldsymbol{u}}{Dt} = \boldsymbol{v}. \end{cases} \tag{3}$$

Again we use $\overline{\overline{\boldsymbol{g}}} = \zeta \overline{\overline{\boldsymbol{\varepsilon}}}$.

Equations

We discretize as before. However, there are nonlinear terms arising from the strain evolution equations. These are linearized using Picard iterations.

$$
\begin{aligned}
N_x(\boldsymbol{v}_k)_{e,t} &= \int_{e,t} \varphi_i \varphi_j \frac{\partial v_k^h}{\partial x} \, d\Omega \\
&= \int_{e,t} \varphi_i \varphi_j \sum_{m=1}^{4} (\boldsymbol{v}_k)_m \frac{\partial \varphi_m}{\partial x} \, d\Omega \\
&= \int_{\hat{\Omega}_{el}} \hat{\varphi}_i \hat{\varphi}_j \sum_{m=1}^{4} (\boldsymbol{v}_k)_m (J_{1\cdot}^{-T} \cdot \nabla \hat{\varphi}_m) |\det J| \, d\hat{\Omega} \\
&\approx \sum_{s=1}^{2} \sum_{t=1}^{2} \omega_s \omega_t \hat{\varphi}_i(\xi_s, \eta_t) \hat{\varphi}_j(\xi_s, \eta_t) |\det J(\xi_s, \eta_t)| S(\xi_s, \eta_t),
\end{aligned}
$$

Equations

We discretize as before. However, there are nonlinear terms arising from the strain evolution equations. These are linearized using Picard iterations.

- Equations are discretized in space using quadrilateral bilinear FE and in time using backward Euler (implicit).
- It can be proven that the strain tensor remains symmetric. We can thus omit one of the equations for $\varepsilon_{12}, \varepsilon_{21}$.

Two brief movies.

Content

1. Motivation
2. Concept of Morphoelasticity
3. 1D Morphoelasticity
4. 2D Viscoelasticity
5. 2D Morphoelaticity
6. Extended Multi-Species Model
7. Future Work

Constitutive equations

Coupled with the morphoelasticity equations, we will now keep track of four concentrations in our tissue: fibroblasts N, myofibroblasts M, generic signalling molecule c and density of collagen molecules ρ.

$$\begin{cases} \dfrac{Dz_i}{Dt} + z_i\,(\nabla \cdot \boldsymbol{v}) = -\nabla \cdot \boldsymbol{J}_i + R_i \quad \text{in } \Omega_t \times [0,T], \\ \dfrac{D(\rho_t \boldsymbol{v})}{Dt} + \rho_t \boldsymbol{v}(\nabla \cdot \boldsymbol{v}) = \nabla \cdot \overline{\overline{\boldsymbol{\sigma}}} + \boldsymbol{f} \quad \text{in } \Omega_t \times [0,T], \\ \dfrac{D\overline{\overline{\boldsymbol{\varepsilon}}}}{Dt} + \overline{\overline{\boldsymbol{\varepsilon}}}\,\text{skw}(\nabla \boldsymbol{v}) - \text{skw}(\nabla \boldsymbol{v})\overline{\overline{\boldsymbol{\varepsilon}}} + \big(\text{Tr}(\overline{\overline{\boldsymbol{\varepsilon}}}) - 1\big)\,\text{sym}(\nabla \boldsymbol{v}) = -\overline{\overline{\boldsymbol{g}}} \\ \text{in } \Omega_t \times [0,T], \end{cases} \tag{4}$$

where z_i is the concentration of each cell constituent $i \in \{N, M, c, \rho\}$.

Fibroblasts and Myofibroblasts

$$\frac{Dz_i}{Dt} + z_i\left(\nabla \cdot \boldsymbol{v}\right) = -\nabla \cdot \boldsymbol{J}_i + R_i$$

$$\begin{aligned}
\boldsymbol{J}_N &= -D_F F \nabla N + \chi_F N \nabla c,\\
\boldsymbol{J}_M &= -D_F F \nabla M + \chi_F M \nabla c,\\
R_N &= r_F \left[1 + \frac{r_F^{\max} c}{a_c^I + c}\right]\left[1 - \kappa_F F\right] N^{1+q} - k_F c N - \delta_N N,\\
R_M &= r_F \left\{\frac{\left[1 + r_F^{\max}\right] c}{a_c^I + c}\right\}\left[1 - \kappa_F F\right] M^{1+q} + k_F c N - \delta_M M,
\end{aligned}$$

where $F = M + N$.

Signalling Molecule

$$\frac{Dz_i}{Dt} + z_i\left(\nabla \cdot \boldsymbol{v}\right) = -\nabla \cdot \boldsymbol{J}_i + R_i$$

$$\boldsymbol{J}_c = -D_c \nabla c,$$

$$R_c = k_c \left[\frac{c}{a_c^{II} + c}\right]\left[N + \eta^I M\right] - \delta_c g(N, M, c, \rho) c,$$

Collagen Density

$$\frac{Dz_i}{Dt} + z_i \left(\nabla \cdot \boldsymbol{v}\right) = -\nabla \cdot \boldsymbol{J}_i + R_i$$

$$\boldsymbol{J}_\rho = \boldsymbol{0},$$

$$R_\rho = k_\rho \left\{1 + \left[\frac{k_\rho^{\max} c}{a_c^{IV} + c}\right]\right\} \left[N + \eta^I M\right] - \delta_\rho g(N, M, c, \rho)\rho.$$

Momentum and Strain Evolution Forces

$$\frac{D(\rho_t \boldsymbol{v})}{Dt} + \rho_t \boldsymbol{v}(\nabla \cdot \boldsymbol{v}) = \nabla \cdot \overline{\overline{\boldsymbol{\sigma}}} + \boldsymbol{f}$$

$$\boldsymbol{f} = \nabla \cdot \boldsymbol{\psi}$$

$$\boldsymbol{\psi} = \xi M \frac{\rho}{R^2 + \rho^2} \boldsymbol{I}.$$

$$\frac{D\overline{\overline{\boldsymbol{\varepsilon}}}}{Dt} + \overline{\overline{\boldsymbol{\varepsilon}}}\,\mathrm{skw}(\nabla \boldsymbol{v}) - \mathrm{skw}(\nabla \boldsymbol{v})\overline{\overline{\boldsymbol{\varepsilon}}} + \big(\mathrm{Tr}(\overline{\overline{\boldsymbol{\varepsilon}}}) - 1\big)\,\mathrm{sym}(\nabla \boldsymbol{v}) = -\overline{\overline{\boldsymbol{g}}}$$

The rate of change of the strain tensor is given by:

$$\overline{\overline{\boldsymbol{g}}} = \zeta \left[\frac{g(N, M, c, \rho)c}{\rho} \right] \overline{\overline{\boldsymbol{\varepsilon}}} = \zeta \left\{ \frac{\left[N + \eta^{II} M\right] c}{1 + a_c^{III} c} \right\} \overline{\overline{\boldsymbol{\varepsilon}}}.$$

Nonlinearity and Source/Sink Separation

- Nonlinear terms are again linearized using Picard iterations.
- To ensure positivity of the non-negative variables we apply Patankar's source/sink separation technique. Consider a PDE of the unknown u of the form $L(u) + S = 0$. Let S be the source term (for us it will be $-R_i$), we consider its source $S_1 > 0$ and sink $S_2 > 0$ parts s.t. $S = S_1 - S_2$. The proposed technique sets

$$S = S_1 - \frac{S_2}{u} u \approx S_1 - \frac{S_2}{u^*} u.$$

Nonlinearity and Source/Sink Separation

Since for our set of equations the term $S = S(u) = S_1(u) - S_2(u)$, this steps would lead to nonlinearity. As such we first set $S = S(u) \approx S(u^*)$ and then proceed with Patankar's technique. We show as an example when it is applied to R_N:

$$-R_N \approx -R_N^* = \underbrace{-r_F \left[1 + \frac{r_F^{\max} c}{a_c^I + c}\right] [1 - \kappa_F F] \, N^{*1+q}}_{-S_2} + \underbrace{k_F c N^* + \delta_N N^*}_{S_1},$$

$$\text{Patankar:} \quad - r_F \left[1 + \frac{r_F^{\max} c}{a_c^I + c}\right] [1 - \kappa_F F] \, N^{*1+q} \frac{N}{N^*} + k_F c^* N^* + \delta_N N^*,$$

$$\text{Picard:} \quad - r_F \left[1 + \frac{r_F^{\max} c^*}{a_c^I + c^*}\right] [1 - \kappa_F F^*] \, N^{*1+q} \frac{N}{N^*} + k_F c^* N^* + \delta_N N^*;$$

Stabilization

- Convection-diffusion equations can give rise to spurious oscillations in the solution. These are detrimental to the quality of our solution, especially given the restriction of being always-positive.

Stabilization

- Convection-diffusion equations can give rise to spurious oscillations in the solution. These are detrimental to the quality of our solution, especially given the restriction of being always-positive.
- Different stabilization techniques can be applied to avoid this. In the paper of V. John and E. Schmeyer, *Finite element methods for time-dependent convection–diffusion–reaction equations with small diffusion (2008)* a comparison among common techniques has been made and the most promising appears to be the algebraic flux correction.

Positivity Preserving Algebraic Flux Correction

In the paper of O. Boiarkine et al, *A positivity-preserving ale finite element scheme for convection–diffusion equations in moving domains* an algorithm is proposed which appears to be well suited for our problem. The main steps are:

- Construct a positivity preserving low order solution of the problem by manipulation of the convection matrix. Zero row and column sums to have discrete mass conservation. Time discretization with implicit midpoint rule.

Positivity Preserving Algebraic Flux Correction

In the paper of O. Boiarkine et al, *A positivity-preserving ale finite element scheme for convection–diffusion equations in moving domains* an algorithm is proposed which appears to be well suited for our problem. The main steps are:

- Construct a positivity preserving low order solution of the problem by manipulation of the convection matrix. Zero row and column sums to have discrete mass conservation. Time discretization with implicit midpoint rule.
- Approximate the nodal derivatives.

Positivity Preserving Algebraic Flux Correction

In the paper of O. Boiarkine et al, *A positivity-preserving ale finite element scheme for convection–diffusion equations in moving domains* an algorithm is proposed which appears to be well suited for our problem. The main steps are:

- Construct a positivity preserving low order solution of the problem by manipulation of the convection matrix. Zero row and column sums to have discrete mass conservation. Time discretization with implicit midpoint rule.
- Approximate the nodal derivatives.
- Recover high order solution by adding anti-diffusive terms.

Remarks and Open Questions

- The solution still presents oscillatory components.

Remarks and Open Questions

- The solution still presents oscillatory components.
- We have a strong mesh dependency. Higher resolution leads to smaller oscillations/peaks, but it introduces negative terms which are then suppressed (non positivity-preserving diffusion matrix).

Remarks and Open Questions

- The solution still presents oscillatory components.
- We have a strong mesh dependency. Higher resolution leads to smaller oscillations/peaks, but it introduces negative terms which are then suppressed (non positivity-preserving diffusion matrix).
- θ-time integration method for low order solution is much more diffusive. Why?

Remarks and Open Questions

- The solution still presents oscillatory components.
- We have a strong mesh dependency. Higher resolution leads to smaller oscillations/peaks, but it introduces negative terms which are then suppressed (non positivity-preserving diffusion matrix).
- θ-time integration method for low order solution is much more diffusive. Why?
- In aforementioned comparison paper the flux correction (altough different algorithm) has been applied on all the matrices. Could this improve the quality of the solution and making it less mesh dependent?

Results

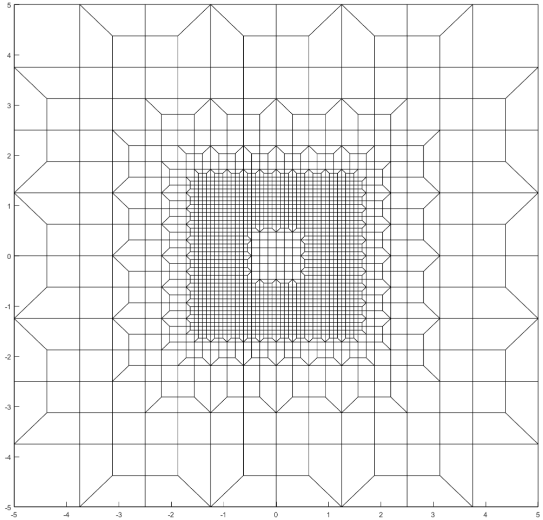

Results

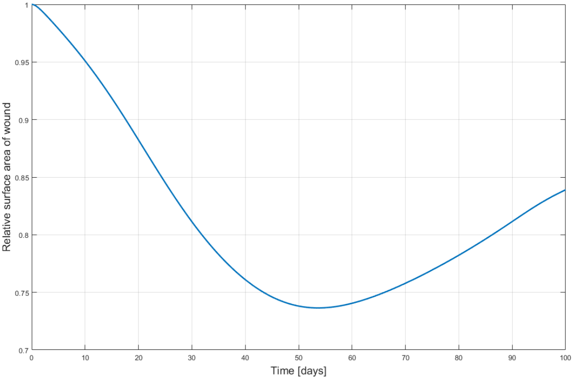

Relative surface area of wound
1
0.95
0.9
0.85
0.8
0.75
0.7
0
10
20
30
40
50
60
70
80
90
100
Time [days]

Content

1. Motivation
2. Concept of Morphoelasticity
3. 1D Morphoelasticity
4. 2D Viscoelasticity
5. 2D Morphoelaticity
6. Extended Multi-Species Model
7. Future Work

Isogeometric Analysis

Next step is to utilize Isogeometric Analysis to solve the problem at hand. In order to achieve this task, we will take advantage of the C++ library G+Smo. G+Smo has specifically been designed to enable efficient and accessible applications of the IGA theory.

- More accurate domain approximation (B-splines). Potentially no error in the discretization of the boundary surface.

Isogeometric Analysis

Next step is to utilize Isogeometric Analysis to solve the problem at hand. In order to achieve this task, we will take advantage of the C++ library G+Smo. G+Smo has specifically been designed to enable efficient and accessible applications of the IGA theory.

- More accurate domain approximation (B-splines). Potentially no error in the discretization of the boundary surface.
- Less need for remeshing.

Isogeometric Analysis

Next step is to utilize Isogeometric Analysis to solve the problem at hand. In order to achieve this task, we will take advantage of the C++ library G+Smo. G+Smo has specifically been designed to enable efficient and accessible applications of the IGA theory.

- More accurate domain approximation (B-splines). Potentially no error in the discretization of the boundary surface.
- Less need for remeshing.
- Reduction in the size of the system of equations while maintaining comparable accuracy to traditional FEM.